enna, Austria, 1968), Vol. 1, p. 267, and Phys. Rev. B 2, 4603 (1970).

[2]J. Skalyo, Jr., B. C. Frazer, and G. Shirane, Phys. Rev. B 1, 278 (1970).

[3]M. Arsic-Eskinja, H. Grimm, and H. Stiller, in *Proceedings of the Fifth IAEA Symposium on Neutron Inelastic Scattering, Grenoble, France, 1972* (International Atomic Energy Agency, Vienna, Austria, 1972), p. 825.

[4]H. Meister, J. Skalyo, Jr., B. C. Frazer, and G. Shirane, Phys. Rev. 184, 550 (1969).

[5]E. J. Samuelsen and D. Semmingsen, to be published.

[6]Y. Uesu and J. Kobayashi, Phys. Status Solidi (a) 34, 475 (1976).

[7]F. Seidl, Tschermak's Mineral. Petrogr. Mitt. 1, 432 (1950).

[8]A. Levstik, R. Blinc, P. Kadaba, S. Čižikow, I. Levstik, and C. Filipič, Solid State Commun. 16, 1339 (1975).

[9]J. W. Lynn, M. Iizumi, G. Shirane, S. A. Werner, and R. B. Saillant, Phys. Rev. B 12, 1154 (1975).

Identification of Shallow Electron Centers in Silver Halides

Shiro Sakuragi and Hiroshi Kanzaki

Institute for Solid State Physics, The University of Tokyo, Roppongi, Minato-ku, Tokyo 106, Japan

(Received 15 April 1977)

On the basis of the excitation-induced absorption spectra in silver halides doped with impurities, two kinds of shallow electron centers are identified. One is an electron bound at a silver interstitial ion and corresponds to the intrinsic electron center in silver halides. Addition of chalcogen impurities enhances the spectra of this origin. The other is an electron bound at substitutional divalent cations, the transition energy of which shifts systematically depending on the kind of impurity.

Transient absorption of pure silver halides during band-to-band excitation at liquid helium temperature was first observed by Brandt and Brown.[1] On the basis of the subsequent studies,[2-4] the optical transition has been interpreted as due to an electron polaron bound in an attractive Coulomb field. The origin of the positive charge center, however, has not yet been identified.

In this Letter we report an observation of zero-phonon bands in silver halides doped with impurities. Firstly, the absorption band observed in a pure crystal is enhanced by addition of chalcogen impurities. This provides evidence that the positive charge center in pure silver halides is a silver interstitial ion. Secondly, substitutional divalent cations produce a new set of absorption bands, the energy of which shifts depending on the kind of impurity. This establishes that the divalent cations can be responsible for shallow electron centers of similar nature.

In the present study, pure crystals are obtained by zone-refining in a halogen atmosphere. Doped crystals are grown in vacuum by the Bridgman method after adding the impurity to zone-refined crystals. The doped samples are rapidly cooled from high temperature (300–350°C in helium atmosphere). This procedure, as well as the low concentration of impurities, is effective in suppressing the spectrum broadening. The impurity concentrations are estimated from the amounts added, and the values for the samples in Figs. 1 and 2 are less than 3×10^{-6} mol for chalcogens and about $(3-9)\times10^{-6}$ for divalent cations.

For infrared measurements, samples 200–250 μm thick are immersed in pumped liquid helium. Total light from a platinum screen source[5] is

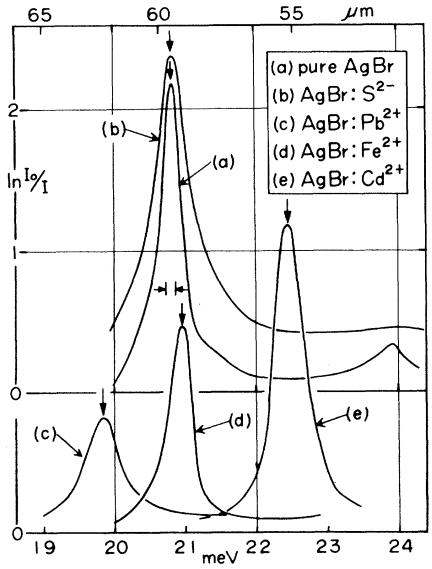

FIG. 1. Typical absorption spectra around zero-phonon band for AgBr doped with impurities during band-to-band excitation at 2 K. The spectral bandwidth used is indicated.

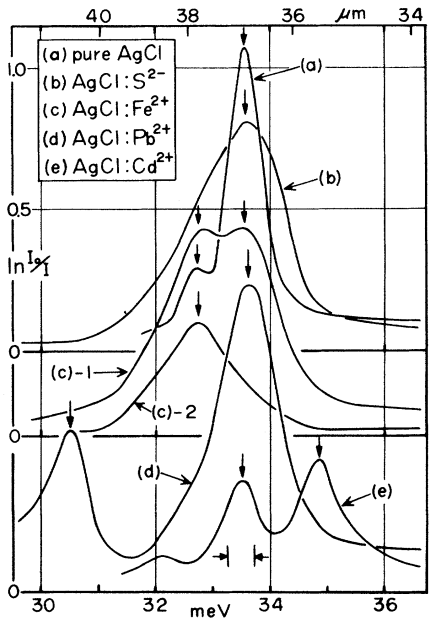

FIG. 2. Typical absorption spectra around zero-phonon band for AgCl doped impurities during band-to-band excitation at 2 K. The excitation intensity in (c)-2 is reduced to about one-twentieth of (c)-1, for the same sample of AgCl:Fe^{2+}. The spectral bandwidth used is indicated

passed through the sample, monochromatized by a grating monochromator, and detected by a germanium bolometer. Band-to-band excitation is provided by a high-pressure mercury lamp through selective filters, and its intensity is fixed in the following data except when otherwise stated. The experimental procedure is to measure first the transmission I_0 without excitation and then the transmission I during excitation. The induced absorption, $\ln(I_0/I)$, obtained corresponds to a steady-state absorption during excitation.

Typical examples of the induced absorption spectra around the zero-phonon band are shown in Figs. 1 and 2, for AgBr and AgCl, respectively.

The result for pure AgBr in Fig. 1(a) agrees with that of Brandt and Brown.[1] It has been established[2,4] that the 20.8-meV band corresponds to $1s$-$2p$ transition of the bound polaron. The 23.9-meV band has been assigned as either $1s$-continuum[1] or $1s$-$3p$.[4] The conductivity modulation spectra[6] suggest the transition from $1s$ to a state close to the continuum.

The result for AgCl in Fig. 2(a) shows stronger absorption compared with the previous data.[1] The 33.5-meV band corresponds to a $1s$-$2p$ transition of intrinsic origin and the weak band at 32.8 meV is due to residual impurity, possibly Fe^{2+}. On the higher energy side, a band at 40.6 meV is assigned as the $1s$-continuum transition.[6]

As shown below, none of the divalent cations reproduce the spectra of the pure crystal. On the other hand, addition of chalcogen, both S^{2-} and Se^{2-}, appreciably enhances the intrinsic absorption band as shown in Figs. 1(b) and 2(b). Furthermore, the decay behavior of induced absorption is not sensitive to chalcogens at the concentration range studied here. Thus it can be concluded that the absorption enhancement is due to the increase in concentration of the positive charge center. As known from ionic conductivity results,[7] the chalcogen ion in silver halides exists as substitutional divalent anion and is accompanied with the increase of silver interstitials. Therefore, the present results strongly suggest that the positive charge in the intrinsic shallow electron center is due to a silver interstitial ion.

Addition of substitutional divalent cations produces zero-phonon bands at energies specific to the impurity. The results give the first direct eivdence of electron trapping by divalent cations in silver halides. The behavior, however, is different for the different halides as follows.

In AgBr, the intrinsic band is hardly observable even at the impurity concentration less than 1×10^{-5}, as shown in Figs. 1(c)–1(e). In AgCl, on the contrary, the intrinsic band always coexists with the extrinsic band, as shown in Figs. 2(c)–2(e). The two kinds of coexisting bands, however, can be easily discriminated by reducing the excitation intensity. As shown typically in Fig. 2(c) for AgCl:Fe^{2+}, the intrinsic band loses its relative strength on reducing the excitation to about one-twentieth from (c)-1 to (c)-2. This phenomenon is related to the difference in their decay behavior and has never been observed in AgBr.

The dependence of the extrinsic band energy on the kind of cation impurity can be explained as follows. It is found that the energy difference between $1s$-$2p$ and $1s$-continuum transitions is the same for all the spectra in the same halide, irrespective of its origin, within experimental error. This corresponds to the shift of the $1s$-$2p$ transition energy being entirely due to the shift of the $1s$ state relative to the conduction band. As in the case of shallow donors in semiconductors,[8,9] the shift can be explained in terms of the central-cell correction to the effective-mass approximation (EMA).

As a first approximation, the central-cell cor-

rection ΔE will be proportional to the effective ionization energy E_i of the core defined as

$$E_i = (\text{second ionization energy of the impurity atom}) - (\text{Madelung energy of the matrix halide}) \quad (1)$$

by considering the divalent impurity at the cation site.

The $1s$-$2p$ zero-phonon transition energy E_0 observed for the cation impurities are plotted against E_i in Fig. 3. Values of Madelung energies used are 8.714 eV (AgBr) and 9.068 eV (AgCl), and those of ionization energies are from Ref. 10. Figure 3 shows that the proportionality holds approximately for impurities having E_i greater than that of Pb^{2+}. The deviation of the Ca^{2+} data may be expected, because the bound electron will not feel the impurity potential in the limit of small E_i and the central-cell correction is reduced to zero. In terms of the EMA, the factor $\Delta E/E_i$ is of the order of the probability of finding the electron in the central cell,[9]

$$\Delta E/E_i \sim (\text{central cell volume})/\pi a^{*3}, \quad (2)$$

where a^* is the effective Bohr radius which is estimated as 19.4 Å (AgBr) and 11.7 Å (AgCl). Taking the central-cell volume as $(\pi/6)(a/2)^3$, where a is the lattice constant, $\Delta E/E_i$ is estimated as 0.55×10^{-3} (AgBr) and 2.3×10^{-3} (AgCl). The values can be favorably compared with the experimental values of $(1\pm0.4)\times10^{-3}$ (AgBr) and $(2\pm0.4)\times10^{-3}$ (AgCl) for the dash-dotted lines in Fig. 3.

The data for intrinsic bands are also included in Fig. 3. Assuming the silver interstitial, the Madelung energy in Eq. (1) is neglected and the first ionization energy of the silver atom (7.576 eV) is taken as E_i. It is shown that the energy of the intrinsic band fits in with the trend of divalent impurities. This will further support the interstitial model of the intrinsic center. For example, if the F-center model (electron at halogen vacancy) is assumed, the Madelung energy term in Eq. (1) turns to positive sign and a deeper localization of electron will be expected.

Two kinds of positive charge centers are thus identified; one is the silver interstitial ion and the other is the divalent cation at a substitutional site. In thermal equilibrium, the concentration of silver interstitials is decreased by adding divalent cations and increased by divalent anions. The present results on AgBr can be explained along this line, and the main origin of interstitials may be frozen-in defects. The situation in AgCl is entirely different, and suggests the production of silver interstitials during band-to-band irradiation of AgCl at low temperature. The type of difference between AgBr and AgCl may be related to the different behavior in exciton self-trapping discussed previously.[11]

Further discussion will be made elsewhere on the experimental results including the multiphonon spectra and also on the deep electron centers observed at higher temperature.

Fruitful discussions with Professor Y. Toyozawa and Dr. Y. Kondo are deeply appreciated.

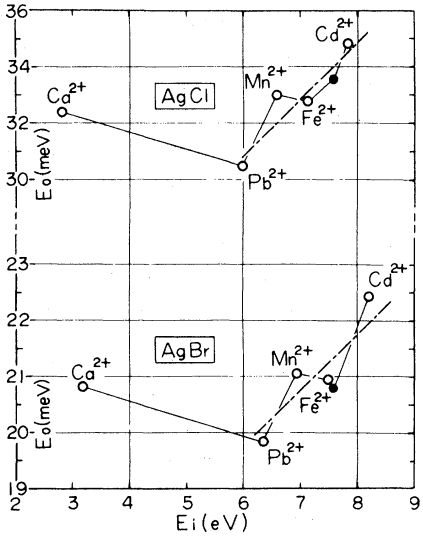

FIG. 3. The $1s$-$2p$ zero-phonon transition energy E_0 vs the effective ionization energy E_i of the core, for the cation impurity centers (○) and the intrinsic center (●). See text for details.

[1]R. C. Brandt and F. C. Brown, Phys. Rev. 181, 1241 (1969).

[2]R. C. Brandt, D. M. Larsen, P. P. Crooker, and G. B. Wright, Phys. Rev. Lett. 23, 240 (1969).

[3]H. Kanzaki and S. Sakuragi, Photo. Sci. Eng. 17, 69 (1973).

[4]K. K. Bajaj and T. D. Clark, Phys. Status Solidi (b) 52, 195 (1972).

[5]D. W. Robinson, J. Opt. Soc. Am. 49, 966 (1959).

[6]H. Kanzaki and S. Sakuragi, in Proceedings of the Conference on Color Centers in Ionic Crystals, Sendai, Japan, August 1974 (to be published).

[7]P. Müller, Phys. Status Solidi 12, 775 (1965).

[8]J. C. Phillips, Phys. Rev. B 1, 1540 (1970).

[9]W. Kohn, in *Solid State Physics*, edited by H. Ehren-

reich, F. Seitz, and D. Turnbull (Academic, New York, 1957), Vol. 5, p. 257.
[10]*American Institute of Physics Handbook* (McGraw-Hill, New York, 1972), 3rd ed., Sec. 7-9.
[11]H. Kanzaki, S. Sakuragi, and K. Sakamoto, Solid State Commun. 9, 999 (1971).

Structure and Electronic Properties of Polymeric Sulfur Nitride $(SN)_x$ Modified by Bromine*

W. D. Gill, W. Bludau, R. H. Geiss, P. M. Grant, R. L. Greene, J. J. Mayerle, and G. B. Street
IBM Research Laboratory, San Jose, California 95193
(Received 11 April 1977)

We report the structure and electronic properties of $(SNBr_{0.4})_x$ and the first chemical modification of the polymeric superconductor $(SN)_x$. Its dc conductivity at 300 K is ten times greater than that for $(SN)_x$ and the thermoelectric power is positive rather than negative. The plasma energy and the superconductivity transition temperature are essentially unchanged. These results suggest that a small displacement of the Fermi level and a large increase in scattering time occur upon bromination.

Since the discovery of the superconducting properties[1] of polymeric sulfur nitride $(SN)_x$ there has been considerable interest in its physical properties and numerous attempts to produce analogous compounds.[2] We have recently succeeded in modifying the properties of $(SN)_x$ films and crystals by reaction with Br_2, I_2, and ICl.[3] Independently, Bernard *et al.*[4] reported on the addition of bromine to $(SN)_x$. In this Letter, we make the first detailed report of the structure and electronic propertites of crystalline $(SN)_x$ reacted with bromine. We find substantial changes in the dc conductivity $\sigma_{dc}(T)$ and the thermoelectric power $S(T)$ while the plasma energy and the superconducting T_c are essentially unchanged. These striking electronic properties are shown to be consistent with an unusual model for bromine incorporation in $(SN)_x$ as suggested by detailed transmission electron microscopy (TEM) results.

On exposure to the vapor pressure of bromine at room temperature, $(SN)_x$ crystals change from gold to blue-black fibrous crystals of composition $(SNBr_{0.5})_x$. Evacuation at 10^{-5} Torr at room temperature for 1 h results in a final composition $(SNBr_{0.4})_x$. At this composition, the crystal has expanded ~ 50% in volume with no measurable expansion in the b direction. During the bromination, some exfoliation and macroscopic cracking is observed. The density increases from 2.32 g/cm^3 to 2.65 g/cm^3.

X-ray precession photographs of individual crystals of $(SNBr_{0.4})_x$ show only $(0k\,0)$ reflections.[3] X-ray powder diffraction results show the $(\bar{1}02)$ reflection of $(SN)_x$ to be broadened, but unshifted, indicating that the a and c lattice constants remain unchanged. TEM diffraction results for $(SN)_x$ and $(SNBr_{0.4})_x$ are shown in Fig. 1. The three most notable features of these data are (1) Bragg diffraction spots appear in approximately the same positions in $(SN)_x$ and $(SNBr_{0.4})_x$; (2) the $(SNBr_{0.4})_x$ pattern shows considerably more streaking perpendicular to b^*; and (3) diffuse lines are observed perpendicular to b^* at $(0\,\frac{1}{2}k\,0)$. Forbidden reflections observed in both patterns are due to multiple diffraction effects. The unchanged Bragg diffraction spots show that the $(SN)_x$ lattice remains unchanged on bromination in agreement with the powder x-ray data. The increased streaking in the diffraction pattern

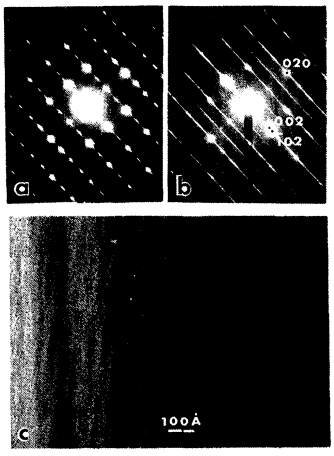

FIG. 1. Electron diffraction pattern from (a) $(SN)_x$ fibers showing the b^*c^* reciprocal lattice net; (b) $(SNBr_{0.4})_x$ fibers oriented similarly to (a). The simultaneous occurrence of (002) and $(\bar{1}02)$ reflections and the larger streaks are attributed to extensive twinning; and (c) electron micrograph of $(SNBr_{0.4})_x$ twinned fibers with 20-Å dimensions.